Synthesis and characterisation of fluorescent aminophosphines
and their coordination to gold(I)

Lara M. Groves,[a] Benjamin D. Ward,[a] Paul D. Newman,[a] Peter N. Horton,[b] Simon J. Coles,[b] Simon J.A. Pope*[a]

a. School of Chemistry, Main Building, Cardiff University, Cardiff CF10 3AT. Fax: (+44) 029-20874030; Tel: (+44) 029-20879316; E-mail: popesj@cardiff.ac.uk.
b. UK National Crystallographic Service, Chemistry, Faculty of Natural and Environmental Sciences, University of Southampton, Highfield, Southampton, SO17 1BJ, England.

Abstract

Three novel fluorescent aminophosphine ligands have been synthesised that incorporate napthyl (**L1**), pyrenyl (**L2**) and anthraquinone (**L3**) chromophores into their structures. The ligands react with [AuCl(tht)] (tht = tetrahydrothiophene) to give neutral complexes of the form [AuCl(**L1-3**)]. Solid state, X-ray crystallographic data was obtained for the anthraquinone derivative, [AuCl(**L3**)], and showed a distorted linear coordination geometry at Au(I). The packing structure also revealed a number of intermolecular π-π interactions that involve the anthraquinone and phenyl units of the aminophosphine ligand. ^{31}P NMR spectroscopic data revealed δ_P values of +42.2 (**L1**), +42.1 (**L2**) and +26.1 (**L3**) ppm, which shifted downfield upon coordination to Au(I) to +64.6, +64.7, and +55.8 ppm, respectively. Supporting TD-DFT studies were able to reproduce the structure and ^{31}P NMR chemical shifts of [AuCl(**L3**)] as well as rationalise the HOMO-LUMO compositions. Photophysical studies showed that the appended fluorophore dominates the absorption and emission properties for the ligands and complexes, with the anthraquinone derivatives showing visible emission at *ca*. 570 nm which was attributed to the intramolecular charge transfer character of the phosphinoaminoanthraquinone fragment.

Introduction

Aminophosphines of the type R_2N-PR_2 (also referred to as aminophosphanes or phosphinous amides) are a well-known class of phosphorus compound.[i,ii] They can be commonly synthesised from a phosphinous chloride (R_2PCl) and a nucleophilic amine in the presence of base. Although, the P-N bond can be quite sensitive to air and moisture, the nitrogen centre does provide opportunities for controlling the physical properties and reactivity of aminophosphines. Interest in aminophosphines has been

primarily driven by their use as reagents to new heterocyclic organophosphorus species, and their application in coordination chemistry (although when compared to phosphine ligands this area is still relatively immature).

Examples of pioneering work on the coordination chemistry of aminophosphines were conducted by Woollins and co-workers.[iii] Synthetic approaches, including those by Dyer, potentially allow access to mixed donor ligands with adaptable chelating properties.[iv] Importantly, complexes that incorporate aminophosphines have been deployed as catalysts for several transformations, including Suzuki-Miyaura,[v] asymmetric hydrosilylation[vi] reactions and allylic alkylations.[vii] Interestingly, Pd(II) complexes of chiral aminophosphines have been used for the enantiodiscrimination of amino acids using ^{31}P NMR spectroscopy.[viii]

In our ongoing studies investigating new ligand architectures that can impart fluorescent properties upon Au(I) coordination complexes[ix], aminophosphines present an ideal class of compound that have yet to be fully explored. Examples are rare, but in the early 2000s Zhang and co-workers reported a series of papers that described the Au(I) coordination chemistry of anthracene-based aminophosphine ligands together with their fluorescence properties.[x] In fact, examples of fluorescent phosphine-based ligands are also relatively sparse. Notable cases include Bodipy-tagged systems developed by Higham[xi] that have been successfully explored in cell imaging work.[xii] The Au(I) complexes of related Bodipy-phosphine dyads have been investigated in gold-catalyzed alkyne transformations.[xiii] Recently, Gabbai has demonstrated that a fluorescein-appended tertiary phosphine can be used as a "sensor" for Au(III) ions by modulating photoinduced electron transfer between the phosphorus atom and fluorophore.[xiv] Other examples of fluorophore-functionalised phosphines have sought to manipulate the reactivity of phosphorus in the detection of reactive oxygen species (ROS).[xv] Similar approaches utilising aminophosphine architectures have not been reported.

In a biological context, a small handful of aminophosphine complexes of gold(I) have been reported in recent years and have shown some promise as antibacterial agents.[xvi] In this current work, we describe our progress in the synthesis and characterisation of fluorescent aminophosphine derivatives and explore their coordination chemistry with Au(I). Our strategy is represented in Scheme 1, wherein the fluorescent component of the ligand is added *via* the choice of amine. We present details of the spectroscopic properties of these species together with an example of a structurally characterised fluorescent aminophosphine Au(I) complex.

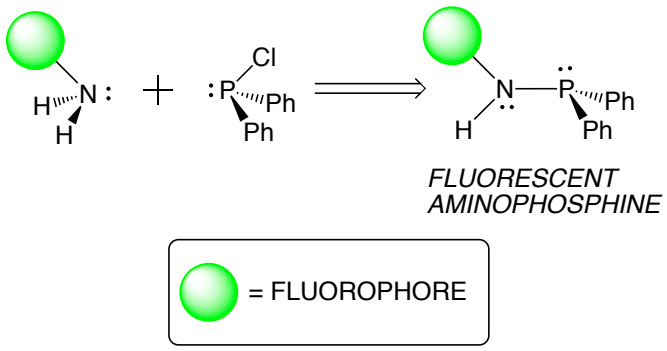

Scheme 1. Cartoon representation of a fluorophore appended aminophosphine.

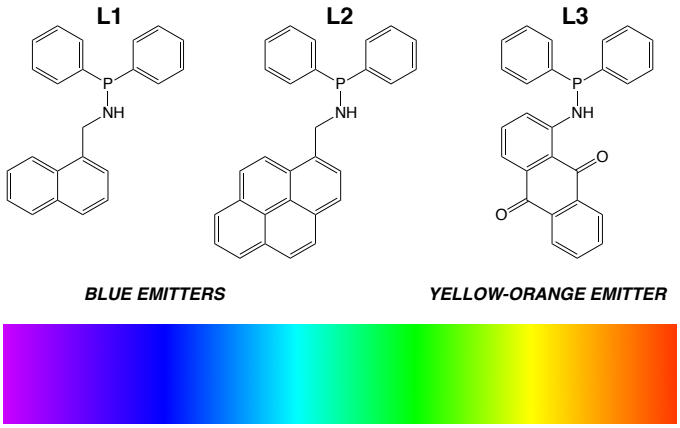

Scheme 2. Structures of the aminophosphine fluorophores isolated in this work.

Results and Discussion

Synthesis

The aminophosphine ligands (**L1**-**L3**) (Scheme 2) were synthesised in a single step from chlorodiphenylphosphine (Ph_2PCl) and the relevant primary amine (1-naphthalenemethylamine, 1-pyrenemethylamine, 1-aminoanthraquinone). The phosphine was added dropwise to a stirred, degassed dichloromethane solution of the amine in the presence of base (triethylamine) at 0 °C. **L1** and **L2** were isolated as colourless and yellow oils, respectively, while the anthraquinone derivative **L3** was obtained as a dark orange solid. The formation of **L3** is noteworthy as the amine of 1-aminoanthraquinone is far less basic, and is delocalised into the strongly electron withdrawing anthraquinone ring. All ligands were assumed to be, and treated as, air/moisture-sensitive materials and were stored under an inert atmosphere. The

corresponding gold(I) complexes were synthesised by stirring [AuCl(tht)] (where tht = tetrahydrothiophene) with the ligand in deoxygenated dichloromethane to yield air-stable species. Further purification of [AuCl(**L3**)] was achieved using column chromatography (silica) without any notable degradation of the product.

Spectroscopic Characterisation of Ligands and Complexes

Multinuclear NMR spectroscopy was used to confirm the proposed structures of the ligands. In the first instance, ^{31}P NMR chemical shift data (Table 1) gave immediate indication of the formation of the target aminophosphine. For structurally related **L1** and **L2**, which incorporate a methylamine unit, this value is approximately +42 ppm, which is comparable to the handful of reports on chemical shift values for $Ph_2(RHN)P$ type species (+40 to +70 ppm).[4] For **L3** the $^{31}P\{^1H\}$ NMR chemical shift value appeared at a relatively upfield value around +26 ppm suggesting that the phosphorus nucleus is more shielded in the aminoanthraquinone derivatives. This value is consistent with the report of Woollins *et al* who described the reactivity of an arylamine with Ph_2PCl to give a corresponding aminophosphine with a recorded ^{31}P NMR resonance at approximately +27 ppm.[xvii]

In the ^{1}H NMR spectra of **L1** and **L2**, the N*H* resonance gave rise to a complex multiplet around 2.3 ppm due to both $^3J_{HH}$ and $^2J_{HP}$ coupling. The methylene resonances for **L1** and **L2** were observed at 4.44 and 4.67 ppm, respectively. In **L3** the N*H* resonance appeared much further downfield at *ca*. 10.3 ppm, due to the strongly electron withdrawing anthraquinone unit, and presented as a doublet, which is attributed to H-P coupling ($^2J_{HP}$ = 7.3 Hz). This is consistent with previous work on substituted aminoanthraquinones which often show such resonances at chemical shifts above 9 ppm.[xviii] For **L3**, the $^{13}C\{^1H\}$ NMR spectrum revealed the two unique carbonyl carbons at 186.4 and 183.5 ppm due to the unsymmetrical nature of the anthraquinone moiety. In **L1** and **L2**, the methylene carbon resonances were noted as doublets ($^2J_{CP}$ ~ 16 Hz) *ca*. 48 ppm, again consistent with the formation of the aminophosphine. The number of aromatic resonances suggest that the phenyl groups are inequivalent (suggesting restricted rotation). High resolution mass spectrometry (HRMS) was obtained for each ligand confirming the proposed formulation. IR spectra

of the ligands allowed identification of ν(N-H) and in the case of **L3**, ν(C=O) stretching frequencies.

Table 1. The ^{31}P NMR chemical shift values for the ligands and complexes. Selected comparative calculated values are included in parentheses.

Compound	^{31}P, δ / ppm	($\delta_{complex}$ - δ_{ligand}) / ppm
L1	+42.2	-
L2	+42.1	-
L3	+26.1 (+26.8)	-
[AuCl(**L1**)]	+64.6	+22.4
[AuCl(**L2**)]	+64.7	+22.6
[AuCl(**L3**)]	+55.8 (+49.9)	+29.7

The Au(I) complexes were similarly characterised with an array of techniques. Firstly, ^{31}P{^{1}H} NMR (Table 1) spectra revealed significant downfield shifts (up to around +30 ppm) for each of the complexes relative to the free ligands, consistent with coordination to Au(I). As with the corresponding ligands, the phosphorus resonances for [AuCl(**L1**)] and [AuCl(**L2**)] were very similar (*ca*. +65 ppm), while [AuCl(**L3**)] appeared around +56 ppm. ^{1}H NMR spectra showed retention of the fluorophore labelled aminophosphine in each case (with the requisite number of aromatic resonances), and for [AuCl(**L1**)] and [AuCl(**L2**)] the methylene resonances were shifted downfield by around +0.2 ppm upon formation of the complexes. These spectra also show the N*H* resonance, again confirming the integrity of the aminophosphine upon coordination to Au(I). For [AuCl(**L3**)] the ^{13}C{^{1}H} NMR spectrum showed a subtle shift in the carbonyl carbon resonances of the anthraquinone unit, while for [AuCl(**L1**)] and [AuCl(**L2**)] the methylene carbon was again noted around 48 ppm. HRMS data was obtained for each of the complexes again supporting their successful formation.

X-ray Crystallography

During the synthesis of the ligands and complexes, diffraction quality crystals of [AuCl(**L3**)] were isolated. These were obtained via recrystallisation from acetonitrile and diethyl ether. Data collection parameters are shown in the Experimental section,

together with supporting bond length and bond angle data (Table 2). The resultant structure of [AuCl(**L3**)] is shown in Figures 1 and 2.

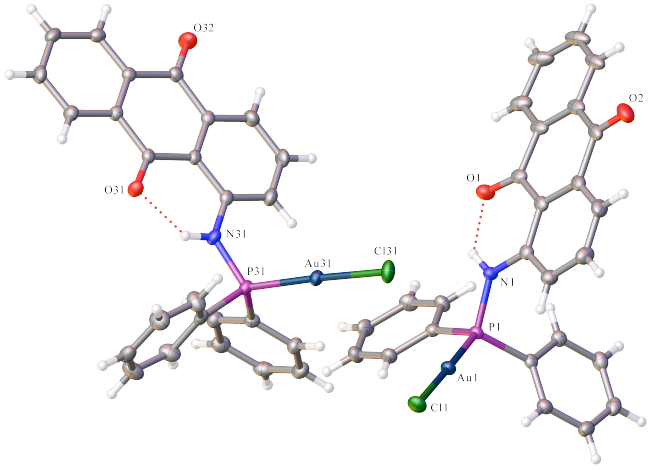

Figure 1. Crystal structure of [AuCl(L3)]. Ellipsoids drawn at 50% probability.

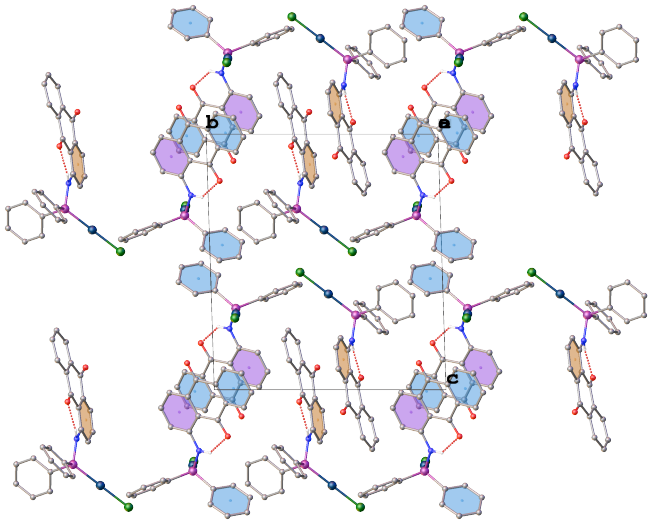

Figure 2. Packing diagram for [AuCl(L3)].

Table 2. Selected bond lengths and bond angles for [AuCl(L3)].

Selected bond lengths (Å)			
Au(1)-Cl(1)	2.2874(5)	Au(31)-Cl(31)	2.2900(6)
Au(1)-P(1)	2.2225(6)	Au(31)-P(31)	2.2224(6)
P(1)-N(1)	1.6774(19)	P(31)-N(31)	1.6851(19)
		Au-Cl	2.356 (calc)
		Au-P	2.296 (calc)
		P-N	1.698 (calc)
Selected bond angles (Å)			
P(1)-Au(1)-Cl(1)	178.38(2)	P(31)-Au(31)-Cl(31)	176.75(2)
N(1)-P(1)-Au(1)	116.88(7)	N(31)-P(31)-Au(31)	117.38(7)

The X-ray crystal structure for [AuCl(**L3**)] confirms the suggested formulation in the solid state (Figure 1). Within the structure there are two independent molecules within the asymmetric unit. The two molecules are very similar to each other, varying by different twist angles for one of the phenyl rings and the anthraquinone (see Figure S1, ESI). The structure reveals the integrity of the anthraquinone functionalised aminophosphine and its coordination to Au(I). The complex adopts an approximately linear coordination geometry at Au(I) with ∠P-Au-Cl in the range 176.75(2)-178.38(2). The Au-P and Au-Cl bond lengths are around 2.22 Å and 2.29 Å, respectively. The P-N distances of 1.6774(19) and 1.6851(19) Å can be regarded as relatively short when compared to other aminophosphines;[1] a previously reported Pt(II) complex of a bis-aminophosphine has a comparable P-N distance of 1.6843(19) Å.[xix]

The structure also reveals intramolecular hydrogen bonding interactions of *ca.* 1.90 Å between the N-H and C=O groups of the anthraquinone moiety. These interactions support the orientation of the P-N bonds which are close to the plane of the anthraquinone (1.73(8)° or 15.55(8)°). The packing arrangement for [AuCl(**L3**)] (Figure 2) revealed intermolecular π-π interactions between the phenyl rings of the anthraquinone unit, and the phenyl rings of the diphenylphosphine moiety (details in table S1, ESI). The closest interactions are between the anthraquinones of neighbouring complex units. There are no aurophilic interactions revealed by this structure, presumably due to the significant steric constraints of the aminophosphine ligand.

The steric properties of **L3** have also been assessed from the crystal data by use of the SambVca 2 program[xx] for determination of buried volume (%V_{bur}) and the method of Mingos[xxi] for deriving crystallographic cone angles. The %V_{bur} values for the two independent molecules in the unit cell are 32.0° and 32.9° respectively, with attendant cone angles of 163° and 169°. These relatively large values reflect the absence of any steric hindrance at the metal (as is typical for a linear L-Au-Cl complex) with the largest values being associated with the complex where both phenyl rings are orthogonal with M-P-C-C torsion angles of 13.3° and 9.9°.

U.V.-vis. absorption properties

Table 3. Absorption and emission data for the ligands and complexes.[a]

Compound	λ_{abs} / nm	λ_{em} / nm	τ_{obs} / ns[b]	ϕ
L1	293, 282, 272, 262, 223	339	6.5	-[c]
L2	375, 344, 328, 314, 300, 276, 266, 242, 235 sh	398, 478	8.0	-[c]
L3	470, 309, 279, 269, 245, 228 sh	571	1.0	-[c]
[AuCl(**L1**)]	291, 282, 272, 223	339	3.9	8 %
[AuCl(**L2**)]	375, 343, 327, 313, 300, 276, 266, 242, 233	377, 397, 417	14.9	17 %
[AuCl(**L3**)]	442, 298, 270, 241, 224	574	1.0	2 %

[a] measurements obtained in MeCN solutions; [b] using λ_{ex} 295 nm; [c] not determined due to potential air-sensitivity in solution.

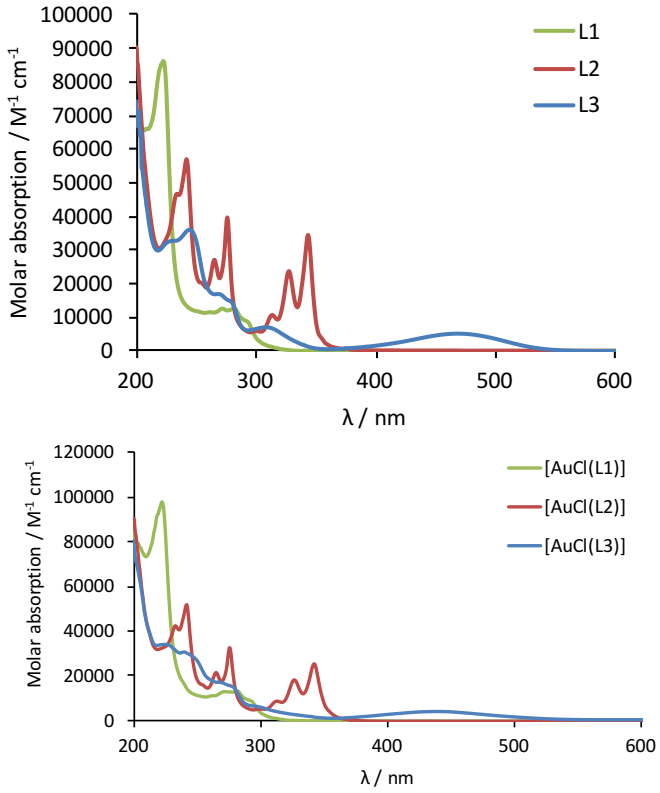

Figure 3. UV-vis. absorption spectra (recorded in MeCN) for the ligands (top) and complexes (bottom).

Solution state (MeCN) UV-vis. absorption spectra were obtained for all ligands and complexes and the data is shown in Table 3. The spectra for the ligands are dominated by $\pi \rightarrow \pi^*$ absorbances (Figure 3) associated with the various aromatic units. The phenyl substituents contribute at the higher energies (<260 nm), while the naphthyl, pyrenyl and anthraquinone chromophores gave additional absorbances at progressively longer wavelengths. For **L2**, the

spectrum revealed a vibronically structured appearance at 300-375 nm, consistent with the various pyrene centred $\pi \rightarrow \pi^*$ transitions. In the case of the anthraquinone derivative **L3**, a lowest energy broad absorption band appeared at 470 nm ($\varepsilon \sim 5000\ M^{-1}cm^{-1}$); this compares with 480 nm (MeOH) for 1-aminoanthraquinone.[xxii] Amine-substituted anthraquinone derivatives are known to possess transitions that can be described as intramolecular charge transfer (ICT)[xxiii] due to the donor-acceptor character of the chromophore. The precise positioning of the ICT band depends upon the nature and positioning of the substituent at the anthraquinone core. Therefore while the 470 nm band is ascribed to an ICT-type transition, it is one that may involve participation from the bonded P atom in the donor component (see later DFT discussion).

For the Au(I) complexes the UV-vis. spectra (Figure 3) were dominated by the ligand-centred transitions discussed above, with minor perturbations observed as a consequence of coordination to Au(I). The case of [AuCl(**L3**)] is noteworthy, as it displays a hypsochromic shift of the ICT visible band upon coordination of Au(I). The shift is consistent with a reduction in the donor ability of the nitrogen atom at anthraquinone and rationalised by the direct conjugation of the gold atom to the anthraquinone unit *via* the P-N bond.

Density Functional Theory

The structures of **L3** and [AuCl(**L3**)] were computed using density functional calculations. Long-range corrected functionals such as CAM-B3LYP[xxiv] are often required for giving an adequate description of excited states with a significant charge-transfer component.[xxv] In this case however, all the TD-DFT analyses (*vide infra*) gave excitation energies that were significantly higher in energy than those observed experimentally. After several functionals were screened, the M06 functional gave good agreement between experiment and theory,[xxvi] and was therefore used throughout. The SDD basis set,[xxvii] along with associated effective core potentials, was used for the Au atom, as is common practice for heavy transition metals; Dunning's correlation-consistent double-ζ basis set cc-pVDZ gave good results (for C, H, O, N) with reasonable computational cost,[xxviii] although the cc-pV(D+d)Z basis set was used for the third period elements, since this gives improved *d*-polarization compared to the

original formulations,[xxix] and is likely to be beneficial in coordination complexes bearing P and Cl donors.

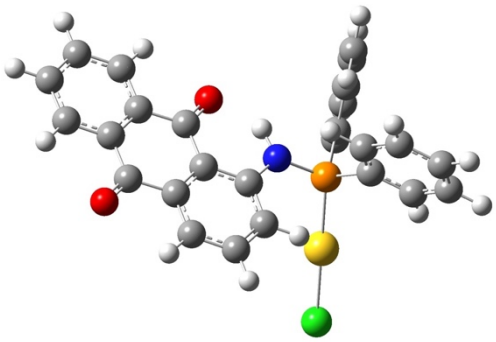

Figure 4. Calculated structure of [AuCl(L3)] [M06 – SDD/cc-pV(D+d)Z/cc-pVDZ]

The calculated structure (optimised coordinates in ESI) of [AuCl(**L3**)] is shown in Figure 4, and is in good agreement with that obtained from X-ray data. The Au-donor distances (see Table 3) are slightly overestimated in the calculated structure (Au–Cl: calculated = 2.356 Å, experimental = 2.2874(5) Å and 2.2900(6) Å; Au–P: calculated = 2.296 Å, experimental = 2.2225(6) Å and 2.2224(6) Å), whilst those within the ligand manifold are more accurately reproduced (*e.g*. P–N: calculated = 1.698 Å, experimental = 1.6774(19) Å and 1.6851(19) Å). The trigonal planar (sp^2-hybridized) amine is well replicated by the calculations (sum of angles subtended at N: calculated = 358.2°, experimental = 360.0° for both independent molecules in the asymmetric unit). The modest differences in bond distance are not thought to be significant in light of crystal packing forces and temperature effects (X-ray data were collected at 100 K), and other properties pertaining to this complex were well-reproduced (*vide infra*).

The ^{31}P NMR shielding tensors were calculated to validate the observed experimental values; this is especially pertinent since there are few literature examples of this molecular fragment to give a reliable "expected" chemical shift range. As noted by Pellegrinet,[xxx,xxxi] the accuracy of such calculations can be improved by ensuring that a suitable reference molecule is chosen and calculated at the same level of theory. Given the structure of **L3** (*i.e*. bearing two phenyl groups), PPh_3 was used, and for which the experimental chemical shift is well established (–6 ppm). These calculations allowed the ^{31}P NMR chemical shifts (see Table 1) of **L3** and [AuCl(**L3**)] to be estimated as +26.8 and +49.9 ppm respectively, in good agreement with the experimental values of +26.1 and +55.8 ppm.

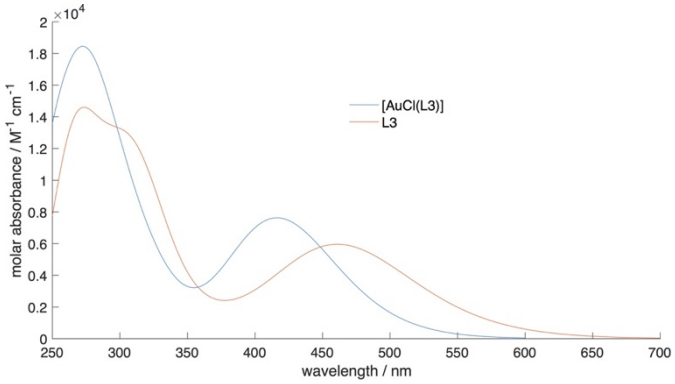

Figure 5. Simulated UV/vis absorption spectra of L3 and [AuCl(L3)] [M06 – SDD/cc-pV(D+d)Z/cc-pVDZ]

The underlying electronic basis of the observed differences in the absorption spectra for **L3** and its Au(I) complex was investigated using TD-DFT calculations. Simulated spectra, derived from the TD-DFT data, are shown in Figure 5, and represent a good agreement with those obtained experimentally. The principal area of interest is the low energy band between 400 and 500 nm, which undergoes a significant blue-shift upon coordination to the Au(I) centre, as observed in the experimental data. As expected, the low energy bands correspond primarily to HOMO-LUMO transitions in both **L3** and [AuCl(**L3**)] (Figures 6 and 7, respectively), and are dominated by significant π-π* character within the substituted anthraquinone. In addition, the HOMO of **L3** contains appreciable orbital coefficients based upon the phosphorus and nitrogen atoms, effectively the P and N lone pairs, which gives the low energy transition a combination of π-π*, n(P)-π*, and n(N)-π* character. The nitrogen orbital component is retained in the HOMO of [AuCl(**L3**)], but the phosphorus orbital character is decidedly altered, as expected, by virtue of coordination of the phosphorus atom to the Au(I) centre; in [AuCl(**L3**)] this component is encompassed in the Au-P σ-bond and thus $\sigma_{Au\text{-}P}$-π* character may also contribute to the HOMO-LUMO transition. Considering the energies of the orbitals involved, the energy of the LUMO is lowered very slightly upon Au coordination, from –2.83 eV in **L3** to –2.98 eV in [AuCl(**L3**)], whereas the corresponding effect on the HOMO is much more pronounced, reducing the energy from –6.29 eV to –6.80 eV. Thus, in effect, the observed blue shift in the absorption spectra is predicted upon lowering of the HOMO upon coordination of the Au(I) ion. All supporting data is included in the ESI.

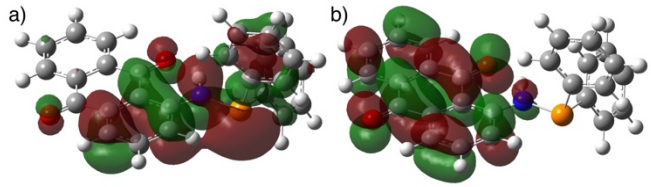

Figure 6. Calculated a) HOMO and b) LUMO of L3 [M06 – SDD/cc-pV(D+d)Z/cc-pVDZ]

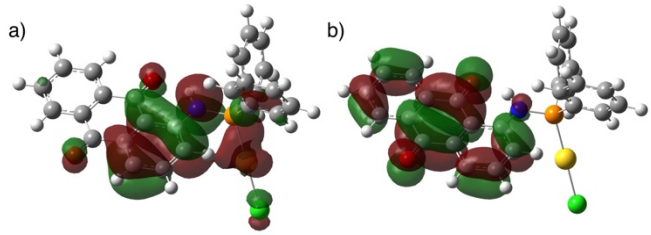

Figure 7. Calculated a) HOMO and b) LUMO of [AuCl(L3)] [M06 – SDD/cc-pV(D+d)Z/cc-pVDZ]

Fluorescence Properties

Each of the ligands was shown to be fluorescent (Figure 8) in aerated acetonitrile solution (2.5×10^{-5} M), with emission wavelengths (Table 3) and profiles consistent with the presence of the organic fluorophore; as anticipated, the emission energy decreased across the series **L1** (naphthyl) > **L2** (pyrene) > **L3** (anthraquinone). In the case of **L2**, the emission profile was composed of both structured monomer-type (350-425 nm) and a broader feature at 475 nm which may be due to excimer-type emission.[xxxii] For **L3**, the visible emission peak at *ca.* 575 nm (λ_{ex} = 440 nm) was broad and structureless in appearance which is consistent with an emitting state of ICT character localised on the aminoanthraquinone moiety. Time-resolved measurements (λ_{ex} = 295 nm) revealed observed lifetimes that were consistent with fluorescence emission in all cases (Table 3). The corresponding measurements on the complexes, using excitation wavelengths that correlate with the ligand-based absorption bands, revealed that the characteristic ligand-based fluorescence (Figure 8) was retained upon complexation to Au(I). For [AuCl(**L2**)] the appearance of the emission profile was highly structured but with no evidence of excimer-type emission. The emission spectra

of **L2** and [AuCl(**L2**)] were obtained using identical concentration solutions (2.5×10^{-5} M), and therefore suggests that the presence of the coordinated {AuCl} unit may inhibit π-π stacking (the excimer band in **L2** may be due to intramolecular interactions between the pyrene and phenyl groups within the ligand). [AuCl(**L3**)] again showed a visible region ICT-based fluorescence band which was subtly shifted, attributed to metal-based perturbation upon Au(I) coordination.

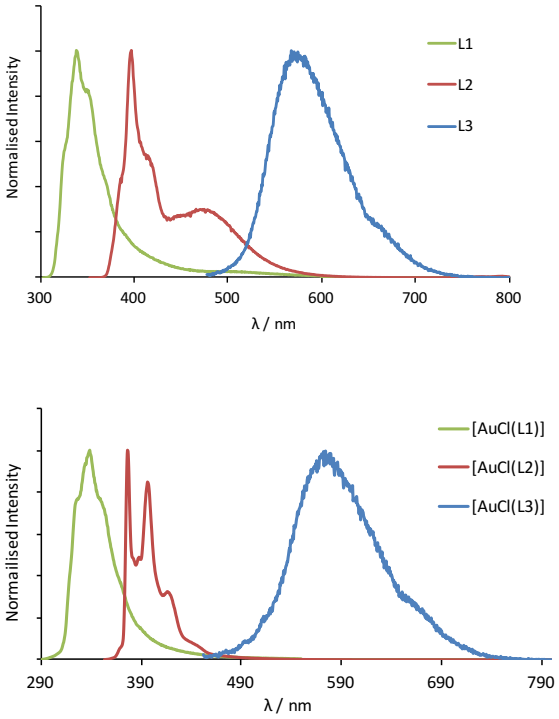

Figure 8. Steady state emission spectra (recorded in MeCN) for the ligands (top) and complexes (bottom).

It is noteworthy that formation of the complexes led to variations in the recorded lifetimes, and in the case of [AuCl(**L2**)] an extension to *ca*. 15 ns. This may indicate that the quenching of the pyrene fluorophore is inhibited by coordination to Au(I). In all cases the observed lifetimes suggest a ligand-centred emission which is fluorescent in nature. Quantum yields were obtained for the complexes using aerated solvent and determined to be 8 %, 17%, and 2% for [AuCl(**L1-3**)], respectively. Therefore, the presence of the Au(I) heavy atom in these complexes does not[xxxiii] result in the observation of room temperature phosphorescence from ligand–centred states, unlike some other Au(I) phosphine complexes.[xxxiv]

Conclusions

Fluorescent, functionalised aminophosphines can be synthesised straightforwardly and coordinated to Au(I) to give air stable complexes. Our examples show that naphthalene, pyrene or anthraquinone type fluorophores can be incorporated into aminophosphine ligand structures. The commercial availability of numerous other fluorescent amines suggests that a large number of fluorescent aminophosphine variants should be accessible. Supporting TD-DFT calculations can reliably reproduce the structural features of the Au(I) complexes. These theoretical approaches can also predict the excitation energies for the anthraquinone derivative and provide further validation via calculated ^{31}P NMR chemical shifts. Our future studies will explore and expand the coordination chemistry of fluorescent aminophosphine ligands and investigate their viability and utility in a broad range of applications including bioimaging and catalysis.

Experimental

General Considerations

All reagents and solvents were commercially available and were used without further purification if not stated otherwise. For the measurement of ^{1}H, ^{31}P, and ^{13}C NMR spectra a Bruker Fourier^{300} (300 MHz), Bruker AVANCE HD III equipped with a BFFO SmartProbe^{TM} (400 MHz) or Bruker AVANCE III HD with BBO Prodigy CryoProbe (500 MHz) was used. The obtained chemical shifts δ are reported in ppm and are referenced to the residual solvent signal. Spin-spin coupling constants *J* are given in Hz.

Low-resolution mass spectra were obtained by the staff at Cardiff University. High-resolution mass spectra were carried out at the EPSRC National Mass Spectrometry Facility at Swansea University. High resolution mass spectral (HRMS) data were obtained on a Waters MALDI-TOF mx at Cardiff University or on a Thermo Scientific LTQ Orbitrap XL by the EPSRC UK National Mass Spectrometry Facility at Swansea University. IR spectra were obtained from a Shimadzu IR-Affinity-1S FTIR.

Reference to spectroscopic data are given for known compounds. UV-Vis studies were performed on a Shimadzu UV-1800 spectrophotometer as MeCN solutions (2.5 or 5 × 10^{-5} M). Photophysical data were obtained on a JobinYvon–Horiba Fluorolog spectrometer fitted with a JY TBX picosecond photodetection module as MeCN solutions. Quantum yield measurements were obtained on aerated MeCN solutions of the complexes using $[Ru(bpy)_3](PF_6)_2$ in aerated MeCN as a standard (Φ = 0.016).[xxxv] Emission spectra were uncorrected and excitation spectra were instrument corrected. The pulsed source was a Nano-LED configured for 295 nm (**L1**, **L2**) or 459 nm (**L3**) output operating at 1 MHz. Luminescence lifetime profiles were obtained using the JobinYvon–Horiba FluoroHub single photon counting module and the data fits yielded the lifetime values using the provided DAS6 deconvolution software.

X-ray Diffraction

A suitable crystal was selected[xxxvi] and mounted on a MITIGEN holder in perfluoroether oil on a Rigaku FRE+ equipped with HF Varimax confocal mirrors and an AFC12 goniometer and HG Saturn 724+ detector diffractometer. The crystal was kept at T = 100(2) K during data collection. Data were measured using profile data from ω-scans using MoK_α radiation. Cell determination, data collection, reduction and absorption correction were carried out using CrystalisPro[xxxvii]. Using Olex2[xxxviii], the structure was solved by charge flipping using *SUPERFLIP*[xxxix] and the models were refined with version 2014/7 of ShelXL[xl] using Least Squares minimisation with all non-H atoms refined anisotropically. Hydrogen atom positions were calculated geometrically and refined using the riding model.

Crystal Data for [AuCl(**L3**)]: $C_{26}H_{18}AuClNO_2P$, M_r = 639.80, triclinic, P-1 (No. 2), a = 9.23605(10) Å, b = 14.82932(17) Å, c = 16.64944(19) Å, α = 90.9323(9)°, β = 101.3732(9)°, γ = 94.2899(9)°, V = 2228.21(4) Å^3, T = 100(2) K, Z = 4, Z' = 2, μ(MoK_α) = 6.819, 60900 reflections measured, 10204 unique (R_{int} = 0.0335) which were used in all calculations. The final wR_2 was 0.0399 (all data) and R_1 was 0.0176 (I > 2(I)).

Density functional calculations

Calculations were undertaken using the Gaussian 09 program,[xli] using the M06 hybrid functional,[xxvi] employing the quasi-relativistic SDD[xxvii] effective core potential along with associated basis set for Au, cc-pV(D+d)Z for Cl and P,[xxix] and cc-pVDZ[xxviii] on all remaining centres. Geometry optimizations were carried out without symmetry restraints, and the nature of the stationary points (minimum or saddle point) verified by calculating the vibrational frequencies. The NMR shielding tensors were calculated using the gauge-including atomic orbital (GIAO) method.[xlii,xliii] Chemical shifts are given relative to PPh_3 calculated at the same level of theory, and calibrated against the experimental chemical shift in $CDCl_3$ (δ = –6.0 ppm). TD-DFT calculations were carried out using the unrestricted M06 functional, with the same basis sets detailed above. The first 20 excited states were calculated; details of all excited states are included in the ESI. Solvent interactions can be crucial for accurately reproducing experimental data;[xxv] solvent was therefore modelled using the polarizable continuum model, with the molecular cavity defined by a united atom model that incorporates hydrogen into the parent heavy atoms, and included in all calculations.[xliv] Geometries were optimized separately in each solvent employed (acetonitrile for TD-DFT and chloroform for NMR shielding tensors) and displayed no significant differences in metric parameters.

Preparation of aminophosphine ligands

Synthesis of L1

1-Naphthalenemethylamine (0.17 ml, 1.4 mmol) and triethylamine (0.19 ml, 1.4 mmol) were dissolved in deaerated dichloromethane (10 ml) under a nitrogen atmosphere. Diphenylchlorophosphine (0.21 ml, 1.4 mmol) in dicloromethane (10ml) was added dropwise at 0 °C over 10 minutes. The resulting solution was stirred at room temperature for 2 hours. The solution was then washed with deaerated water (20 ml), dried over $MgSO_4$ and the solvent removed *in vacuo* to give L1 as a colourless oil (463 mg, 97 %). ^{1}H NMR (400 MHz, $CDCl_3$): δ_H 7.91 – 7.87 (m, 1H), 7.77 (dd, J_{HH} = 6.8, 2.8 Hz, 1H), 7.67 (d, $^3J_{HH}$ = 7.8 Hz, 1H), 7.43-7.34 (m, 7H), 7.34 – 7.24 (m, 7H), 4.44 (app. t, $^3J_{HH}$ = 6.7 Hz, 2H, CH_2), 2.25 – 2.16 (m, 1H, N*H*) ppm. ^{13}C{^{1}H} NMR (101 MHz, $CDCl_3$): δ_C

141.2 (d, J_{CP} = 12.5 Hz), 137.1 (d, J_{CP} = 8.1 Hz), 134.0, 132.3, 132.2, 131.7, 131.5, 129.0, 128.8, 128.7, 128.5, 128.4, 128.0, 126.2, 125.8, 125.7, 125.6, 123.9, 123.3, 48.1 (d, J_{CP} = 16.3 Hz) ppm. $^{31}P\{^{1}H\}$ NMR (162 MHz, $CDCl_3$): δ_P +42.19 ppm. HRMS found *m/z* 342.1400, calcd *m/z* 342.1412 for $[C_{23}H_{20}NP]^+$. UV-vis. (MeCN) λ_{max} (ε / $dm^3mol^{-1}cm^{-1}$): 293 (8520), 282 (12520), 272 (12360), 262, (11280), 223 (86480) nm. IR (solid) ν / cm^{-1}: 3399, 3243, 3049, 1595, 1581, 1508, 1477, 1431, 1390, 1321, 1311, 1261, 1167, 1094, 1082, 1061, 1026, 997, 970, 910, 883, 858, 839, 794, 769, 740, 711, 634, 617, 594, 552, 521, 507, 488, 469, 444, 420, 413.

Synthesis of L2

As with L1, but using 1-pyrenemethylamine (487 mg, 2.1 mmol), triethylamine (0.33 ml, 2.5 mmol), diphenylchlorophosphine (0.38 ml, 2.1 mmol) and dichloromethane (20 ml) to give L2 as a yellow oil (808 mg, 93 %). ^{1}H NMR (400 MHz, $CDCl_3$): δ_H 8.14 – 8.06 (m, 2H), 8.02 – 7.83 (m, 7H), 7.69 (dd, J_{HH} = 11.1, 7.6 Hz, 1H), 7.50 (app. t, J_{HH} = 7.9 Hz, 1H), 7.45 – 7.39 (m, 5H), 7.28 (d, $^{3}J_{HH}$ = 5.1 Hz, 2H), 7.18 – 7.13 (m, 1H), 4.67 (app. t, $^{3}J_{HH}$ = 6.6 Hz, 2H, CH_2), 2.34 – 2.26 (m, 1H, N*H*) ppm. $^{13}C\{^{1}H\}$ NMR (101 MHz, $CDCl_3$): δ_C 141.2 (d, J_{CP} = 12.5 Hz), 135.5 (d, J_{CP} = 7.1 Hz), 135.3 (d, J_{CP} = 7.1 Hz), 134.9 (d, J_{CP} = 8.0 Hz), 131.7, 131.5, 131.4, 130.9 (d, J = 7.9 Hz), 129.7, 129.0, 128.8, 128.7, 128.6, 128.4 (d, J = 6.2 Hz), 127.7, 127.6, 127.5, 126.7, 126.0, 125.2, 125.1, 125.0, 124.9, 123.4, 48.3 (d, J_{CP} = 15.8 Hz) ppm. $^{31}P\{^{1}H\}$ NMR (202 MHz, $CHCl_3$): δ_P +42.12 ppm. HRMS found *m/z* 415.1484, calcd *m/z* 415.1490 for $[C_{29}H_{22}NP]^+$. UV-vis. (MeCN) λ_{max} (ε / $dm^3mol^{-1}cm^{-1}$): 375 (920), 344 (34480), 328 (23800), 314 (10800), 300 (6040), 276 (39680), 266 (27120), 242 (56960), 235 sh (46440) nm. IR (solid) ν / cm^{-1}: 3044, 2963, 2857, 1601, 1585, 1477, 1431, 1414, 1391, 1342, 1306, 1261, 1179, 1173, 1159, 1088, 1067, 1026, 997, 968, 912, 893, 841, 816, 739, 719, 692, 617,586, 555, 513, 419, 409, 401.

Synthesis of L3

As for L1, but using 1-aminoanthraquinone (1 g, 4.6 mmol), triethylamine (0.74 ml, 5.5 mmol), diphenylchlorophosphine (0.85 mmol, 4.6 mmol) and dichloromethane (30 ml) to give L3 as a dark orange solid (583 mg, 64 %). ^{1}H NMR (500 MHz, $CDCl_3$): δ_H 10.36 (d, $^{2}J_{HP}$ = 7.3 Hz, 1H, N*H*), 8.17 – 8.08 (m, 2H), 7.87 – 7.80 (m, 1H), 7.67 – 7.57 (m, 5H), 7.47-7.39 (m, 6H), 7.29-7.26 (m, 2H), 7.12 (s, 1H) ppm. $^{13}C\{^{1}H\}$ NMR (126 MHz, $CDCl_3$):

δ_C 186.4 (C=O), 183.5 (C=O), 152.5, 152.3, 139.0, 138.9, 135.3, 135.2, 134.7, 134.6, 134.2, 133.6, 133.1, 131.5 (d, J_{CP} = 21.3 Hz), 129.7, 128.9 (d, J_{CP} = 7.1 Hz), 127.0 (d, J_{CP} = 16.9 Hz), 126.9, 123.3, 122.8, 122.6, 118.5, 117.4, 116.1 ppm. $^{31}P\{^1H\}$ NMR (162 MHz, $CHCl_3$): δ_P +26.11 ppm. UV-vis. (MeCN) λ_{max} (ε / $dm^3mol^{-1}cm^{-1}$): 470 (4880), 309 (7880), 279 (16160), 269 (18120), 245 (36720), 228 sh (32720) nm. HRMS found *m/z* 408.1167, calcd *m/z* 408.1153 for $[C_{26}H_{19}N_2OP]^+$. IR (solid) ν / cm^{-1}: 3167, 3051, 1668, 1630, 1593, 1570, 1431, 1396, 1346, 1300, 1253, 1231, 1169, 1092, 1070, 1040, 1018, 997, 912, 893, 831, 806, 775, 748, 735, 704, 692, 602, 546, 513, 476, 436, 420.

Preparation of aminophosphine complexes

Synthesis of [AuCl(L1)]

L1 (111 mg, 0.32 mmol) and tetrahydrothiophenegold chloride (94 mg, 0.29 mmol) were added to degassed dichloromethane (20 ml) and the solution stirred at room temperature under nitrogen for 1.5 hours. The solvent was reduced *in vacuo* and hexane added dropwise. The mother liquor was decanted to leave [AuCl(L1)] as a grey solid (35 mg, 21 %). ^1H NMR (400 MHz, $CDCl_3$): δ_H 7.96 (d, $^3J_{HH}$ = 7.9 Hz, 1H), 7.87 (d, $^3J_{HH}$ = 8.4 Hz, 1H), 7.79 (d, $^3J_{HH}$ = 8.2 Hz, 1H), 7.67 (d, $^3J_{HH}$ = 7.5 Hz, 2H), 7.64 (d, $^3J_{HH}$ = 7.4 Hz, 2H), 7.54-7.48 (m, 4H), 7.48-7.42 (m, 5H), 7.42 – 7.36 (m, 1H), 4.71 – 4.64 (m, 2H) ppm. $^{13}C\{^1H\}$ NMR (101 MHz, $CDCl_3$): δ_C 134.1, 132.7, 132.6, 132.4, 132.3, 131.8, 131.2, 129.3, 129.2, 129.1, 129.0, 126.8, 126.7, 126.2, 125.5, 123.4, 47.9 ppm. $^{31}P\{^1H\}$ NMR (162 MHz, $CDCl_3$): δ_P +64.58 ppm. UV-vis. (MeCN) λ_{max} (ε / $dm^3mol^{-1}cm^{-1}$): 291 (9080), 282 (13160), 272 (12920), 223 (97680) nm. HRMS found *m/z* 572.0629, calcd *m/z* 572.0609 for $[C_{23}H_{20}AuClNP]^-$. IR (solid) ν / cm^{-1}: 3248, 3207, 3049, 2359, 1595, 1576, 1555, 1508, 1499, 1476, 1460, 1435, 1395, 1379, 1306, 1265, 1248, 1180, 1167, 1105, 1063, 1041, 1026, 995, 962, 881, 854, 800, 789, 770, 745, 714, 691, 619.

Synthesis of [AuCl(L2)]

L2 (267 mg, 0.64 mmol) and tetrahydrothiophenegold chloride (187 mg, 0. 58 mmol) were added to degassed dichloromethane (20 ml) and the solution stirred at room temperature under nitrogen for 2 hours. The solvent was reduced *in vacuo* and diethyl

ether added dropwise. The resultant precipitate was filtered and dried to yield [AuCl(L2)] as a pale yellow solid (50 mg, 13 %). ^{1}H NMR (500 MHz, $CDCl_3$): δ_H 8.15 – 8.10 (m, 3H), 8.05 (d, $^{3}J_{HH}$ = 9.2 Hz, 1H), 7.99 (d, $^{3}J_{HH}$ = 8.9 Hz, 1H), 7.95 (s, 1H), 7.87 (d, $^{3}J_{HH}$ = 7.7 Hz, 1H), 7.74 (dd, J_{HH} = 13.9, 7.1 Hz, 2H), 7.62 – 7.56 (m, 4H), 7.41 – 7.37 (dd, J_{HH} = 7.4, 1.8 Hz, 1H), 7.36 – 7.31 (m, 3H), 7.23 (app. t, J_{HH} = 7.2 Hz, 2H), 4.83 (dd, J_{HH} = 8.8, 6.4 Hz, 1H), 2.75 (br. s, 1H, N*H*) ppm. ^{13}C{^{1}H} NMR (101 MHz, $CDCl_3$): δ_C 134.3, 133.1, 132.7, 132.5, 132.3, 132.2, 131.4, 130.8, 129.4, 129.3, 129.2, 128.9, 128.6, 128.0, 127.9, 127.8, 127.5, 127.2, 126.3, 125.7, 125.6, 125.0, 124.9, 124.8, 122.8, 122.7, 119.8, 48.2 ppm. ^{31}P{^{1}H} NMR (202 MHz, $CDCl_3$): δ_P +64.72 ppm. UV-vis. (MeCN) λ_{max} (ε / $dm^3mol^{-1}cm^{-1}$): 375 (200), 343 (25280), 327 (18120), 313 (8640), 300 (5080), 276 (32480), 266 (21240), 242 (51680), 233 (42280) nm. HRMS found *m/z* 612.1143, calcd *m/z* 612.1150 for $[C_{29}H_{22}AuNP]^+$. IR (solid) ν / cm^{-1}: 3379, 3036, 2363, 1605, 1587, 1553, 1504, 1499, 1477, 1435, 1418, 1395, 1375, 1304, 1240, 1180, 1169, 1130, 1101, 1067, 1049, 1022, 995, 961, 920, 903, 878, 843, 825, 820, 808, 746, 723, 710, 692, 619.

Synthesis of [AuCl(L3)]

L3 (130 mg, 0.32 mmol) and tetrahydrothiophenegold chloride (93 mg, 0.29 mmol) were added to degassed dichloromethane (15 ml) and the solution stirred at room temperature under nitrogen for 2 hours. The solvent was reduced *in vacuo* and diethyl ether added dropwise. The resultant precipitate was filtered and dried to give a crude solid. This was then purified by column chromatography (silica) and eluted as the first fraction from 9:1 DCM:MeOH, to give [AuCl(L3)] as an orange solid (13 mg, 19 %). ^{1}H NMR (500 MHz, $CDCl_3$): δ_H 10.92 (d, $^{2}J_{HP}$ = 6.1 Hz, 1H, N*H*), 8.31 – 8.24 (m, 2H), 7.95 (d, $^{3}J_{HH}$ = 7.4 Hz, 1H), 7.89 – 7.83 (m, 4H), 7.80 (dd, J_{HH} = 5.9, 2.1 Hz, 2H), 7.67 (d, J_{HH} = 8.0 Hz, 1H), 7.64 – 7.60 (m, 3H), 7.60 – 7.55 (m, 4H) ppm. ^{13}C{^{1}H} NMR (126 MHz, $CDCl_3$): δ_C 187.5, 182.7, 146.6, 135.9, 134.7, 134.6, 134.5, 134.1, 133.2, 133.1, 132.7, 132.6 (d, *J* = 16.1 Hz) 130.3, 129.8 (d, *J* = 12.7 Hz), 127.3, 122.8 (d, *J* = 13.8 Hz), 121.0, 118.0, 117.9 ppm. ^{31}P{^{1}H} NMR (162 MHz, $CDCl_3$): δ_P +55.77 ppm. HRMS found *m/z* 604.0791, calcd *m/z* 604.0735 for $[C_{26}H_{18}AuClNO_2P+Cl]^+$. UV-vis. (MeCN) λ_{max} (ε / $dm^3mol^{-1}cm^{-1}$): 442 (3720), 298 (6040), 270 (16560), 241 (30240), 224 (33760) nm. IR (solid) ν / cm^{-1}: 3410, 3306, 3042, 2976, 2587, 2496, 2374, 1165, 1632, 1585, 1543, 1472, 1460, 1435,

1396, 1344,1265, 1298, 1233, 1171, 1159, 1105, 1042, 1022, 997, 829, 802, 777, 748, 735, 695, 640, 606.

Acknowledgements

We thank the staff of the EPSRC Mass Spectrometry National Service (Swansea University) and the National Crystallographic Service at the University of Southampton. Access to the Cardiff University high performance computing facility "ARCCA" is gratefully acknowledged.

Notes and references

‡ CCDC reference number 1571819 contains the supplementary crystallographic data for this paper. These data can be obtained free of charge from the Cambridge Crystallographic Data Centre *via* www.ccdc.cam.ac.uk/data_request/cif.

[i] M. Alajarin, C. Lopez-Leonardo, P. Llamas-Lorente, *Top Curr. Chem*., 2005, **250**, 77.

[ii] J. Gopalakrishnan, *Appl. Organomet. Chem*., 2009, **23**, 291

[iii] For example: T.Q. Ly, A.M.Z. Slawin, J.D. Woollins, *J. Chem. Soc., Dalton Trans*., 1997, 1611; S.M. Aucott, A.M.Z. Slawin, J.D. Woollins, *Eur. J. Inorg. Chem*., 2002, 2408.

[iv] For example: A.D. Burrows, M.F. Mahon, M.T. Palmer, *J. Chem. Soc., Dalton Trans*., 2000, 3615; S. Naik, S. Kumar, J.T. Mague, M.S. Balakrishna, *Dalton Trans*., 2016, **45**, 18434; L. Baiget, A.S. Batsanov, P.W. Dyer, M.A. Fox, M.J. Hanton, J.A.K. Howard, P.K. Lane, S.A. Solomon, *Dalton Trans*., 2008, 1043; P.W. Dyer, J. Fawcett, M.J. Hanton, *J. Organomet. Chem*., 2005, 690, 5264; P.W. Dyer, J. Fawcett, M.J. Hanton, *Organometallics*, 2008, **27**, 5082; F. Majoumo-Mbe, P. Lonnecke, E. Hey-Hawkins, *Z. Anorg. Allg. Chem*., 2008, **634**, 2385.

[v] M.L. Clarke, D.J. Cole-Hamilton, J.D. Woollins, *J. Chem. Soc., Dalton Trans.*, 2001, 2721

[vi] H. Brunner, H. Weber, Chem. Ber., 1985, **118**, 3380

[vii] X. Chen, R. Guo, Y. Li, G. Chen, C-H. Yeung, A.S.C. Chan, *Tetrahedron: Asymmetry*, 2004, **15**, 213.

[viii] S. Nieto, C. Cativiela, E.P. Urriolabeitia, *New J. Chem*., 2012, **36**, 566.

[ix] L.A. Mullice, F.L. Thorp-Greenwood, R.H. Laye, M.P. Coogan, B.M. Kariuki, S.J.A. Pope, *Dalton Trans*., 2009, 6836; L.A. Mullice, H.J. Mottram, A.J. Hallett, S.J.A. Pope, *Eur. J. Inorg. Chem*., 2012, 3054; E.E. Langdon-Jones, D. Lloyd, A.J. Hayes, S.D. Wainwright, H.J. Mottram, S.J. Coles, P.N. Horton, S.J.A. Pope, *Inorg. Chem*., 2015, **54**, 6606; E.E. Langdon-Jones, S.J.A. Pope, *Chem. Commun*., 2014, **50**, 10343; R.G. Balasingham, C.F. Williams, H.J. Mottram, M.P. Coogan, S.J.A. Pope, *Organometallics*, 2012, **31**, 5835.

[x] F-B. Xu, L-H. Weng, L-J. Sun, Z-Z. Zhang, *Organometallics*, 2000, **19**, 2658; F-B. Xu, Q-S. Li, L-Z. Wu, X-B. Leng, Z-C. Li, X-S. Zeng, Y.L. Chow, Z-Z. Zhang, *Organometallics*, 2003, **22**, 633; Q-S. Li, C-Q. Wan, R-Y. Zou, F-B. Xu, H-B. Song, X-J. Wan, Z-Z. Zhang, *Inorg. Chem*., 2006, **45**, 1888.

[xi] L.H. Davies, B. Stewart, R.W. Harrington, W. Clegg, L.J. Higham, *Angew. Chemie Int. Ed.*, 2012, **124**, 5005.

[xii] S. Nigam, B.P. Burke, L.H. Davies, J. Domarkas, J.F. Wallis, P.G. Waddell, J.S. Waby, D.M. Benoit, A-M. Seymour, C. Cawthorne, L.J. Higham, S.J. Archibald, *Chem. Commun*., 2016, **52**, 7114

[xiii] O. Halter, R. Vasiuta, I. Fernandez, H. Plenio, *Chem. Eur. J*., 2016, **22**, 18066.

[xiv] A.M. Christianson, F.P. Gabbai, *Inorg. Chem*., 2016, **55**, 5828.

[xv] For example: S. Yamaguchi, S. Akiyama, K. Tamao, *J. Organomet. Chem*., 2002, **652**, 3; S. Yamaguchi, S. Akiyama, K. Tamao, *J. Organomet. Chem*., 2002, **646**, 277; T. Hatakeyama, S. Hashimoto, M. Nakamura, *Org. Lett*., 2011, **13**, 2130; J. Wang, Q. Zhao, C.M. Lawson, G.M. Gray, *Opt. Commun*., 2011, **284**, 3090; K. Akasaka, T. Suzuki, H. Ohrui, H. Meguro, *Anal. Lett*., 1987, **20**, 731; M. Onoda, S. Uchiyama, A. Endo, H. Tokuyama, T. Santa, K. Imai, *Org. Lett*., 2003, **5**, 1459; N. Soh, O. Sakawaki, K. Makihara, Y. Odo, T. Fukaminato, T. Kawai, M. Irie, T. Imato, *Bioorg. Med. Chem*., 2005, **13**, 1131; G.A. Lemieux, C.L. de Graffenried, C.R. Bertozzi, *J. Am. Chem. Soc*., 2003, **125**, 4708.

[xvi] L. Ortego, J. Gonzalo-Asensio, A. Laguna, M.D. Villacampa, M.C. Gimeno, *J. Inorg. Biochem*., 2015, **146**, 19; M.F. Fillat, M.C. Gimeno, A. Laguna, E. Latorre, L. Ortego, M.D. Villacampa, *Eur. J. Inorg. Chem*., 2011, 1487.

[xvii] Q. Zhang, G. Hua, P. Bhattacharyya, A.M.Z. Slawin. J.D. Woolins, *Dalton Trans*., 2003, 3250.

[xviii] J.E. Jones, B.M. Kariuki, B.D. Ward, S.J.A. Pope, *Dalton. Trans*., 2011, **40**, 3498.

[xix] M.R.I. Zubiri, H.L. Milton, D.J. Cole-Hamilton, A.M.Z. Slawin, J.D. Woollins, *Polyhedron*, 2004, **23**, 693.

[xx] L. Falivene, R. Credendino, A. Poater, A. Petta, L. Serra, R. Oliva, V. Scarano, L. Cavallo, *Organometallics*, 2016, **35**, 2286

[xxi] T.E. Müller, M.P. Mingos, *Transiton Met. Chem*., 1995, 20, 533

[xxii] Z. Yoshida, F. Takabayashi, *Tetrahedron*, 1968, 24, 913.

[xxiii] E.E. Langdon-Jones, S.J.A. Pope, *Coord. Chem. Rev*., 2014, **269**, 32.

[xxiv] T. Yanai, D.P. Tew, N.C. Handy, *Chem. Phys. Lett.,* 2004, **393**, 51.

[xxv] A. Vlček, S. Záliš, *Coord. Chem. Rev.,* 2007, **251**, 258.

[xxvi] Y. Zhao, D.G. Truhlar, *Theor. Chem. Acc.,* 2008, **120**, 215.

[xxvii] D. Andrae, U. Häußermann, M. Dolg, H. Stoll, H. Preuß, *Theor. Chim. Acta,* 1990, **77**, 123.

[xxviii] T.H. Dunning, *J. Chem. Phys.,* 1989, **90**, 1007.

[xxix] T.H. Dunning, K.A. Peterson, A.K. Wilson, *J. Chem. Phys.,* 2001, **114**, 9244.

[xxx] A.M. Sarotti, S.C. Pellegrinet, *J. Org. Chem.,* 2009, **74**, 7254.

[xxxi] A.M. Sarotti, S.C. Pellegrinet, *J. Org. Chem.,* 2012, **77**, 6059.

[xxxii] B. Bodenant, F. Fages, M.-H. Delville, *J. Am. Chem. Soc*., 1998, **120**, 7511; S.J.A. Pope, *Polyhedron*, 2007, **26**, 4818.

[xxxiii] L.A. Mullice, F.L. Thorp-Greenwood, R.H. Laye, M.P. Coogan, B.M. Kariuki, S.J.A. Pope, *Dalton Trans*., 2009, 6836

[xxxiv] For example: S. Marpu, Z. Hu, M. A. Omary, *Langmuir*, 2010, **26**, 15523

[xxxv] M. Frank, M. Nieger, F. Vogtle, P. Belser, A. von Zelewsky, L. De Cola, V. Balzani, F. Barrigelletti, L. Flamigni, *Inorg. Chim. Acta*, 1996, **242**, 281.

[xxxvi] S.J. Coles, P.A. Gale, *Chem. Sci*., 2012, **3**, 683

[xxxvii] CrysAlisPro Software System, Rigaku Oxford Diffraction, Yarnton, Oxford, UK (2015).

[xxxviii] O.V. Dolomanov, L.J. Bourhis, R.J. Gildea, J.A.K. Howard, H. Puschmann, *J. Appl. Cryst.*, 2009, **42**, 339.

[xxxix] L. Palatinus, G. Chapuis, *J. Appl. Cryst*., 2007, **40**, 786.

[xl] G.M. Sheldrick, *Acta Cryst.*, 2015, C27, 3.

[xli] M.J. Frisch, G.W. Trucks, H.B. Schlegel, G.E. Scuseria, M.A. Robb, J.R. Cheeseman, G. Scalmani, V. Barone, B. Mennucci, G.A. Petersson, H. Nakatsuji, M. Caricato, X. Li, H.P. Hratchian, A.F. Izmaylov, J. Bloino, G. Zheng, J.L. Sonnenberg, M. Hada, M. Ehara, K.

Toyota, R. Fukuda, J. Hasegawa, M. Ishida, T. Nakajima, Y. Honda, O. Kitao, H. Nakai, T. Vreven, J.A. Montgomery Jr, J.E. Peralta, F. Ogliaro, M. Bearpark, J.J. Heyd, E. Brothers, K.N. Kudin, V.N. Staroverov, T. Keith, R. Kobayashi, J. Normand, K. Raghavachari, A. Rendell, J.C. Burant, S.S. Iyengar, J. Tomasi, M. Cossi, N. Rega, J.M. Millam, M. Klene, J.E. Knox, J.B. Cross, V. Bakken, C. Adamo, J. Jaramillo, R. Gomperts, R.E. Stratmann, O. Yazyev, A.J. Austin, R. Cammi, C. Pomelli, J.W. Ochterski, R.L. Martin, K. Morokuma, V.G. Zakrzewski, G.A. Voth, P. Salvador, J.J. Dannenberg, S. Dapprich, A.D. Daniels, O. Farkas, J.B. Foresman, J.V. Ortiz, J. Cioslowski, D.J. Fox, *Gaussian 09, Revision C.01*; Gaussian 09, Revision C.01; Gaussian Inc.: Wallingford CT, 2010.

[xlii] R. Ditchfield, *J. Chem. Phys.,* 1972, **56**, 5688.

[xliii] A.M. Lee, N.C. Handy, S.M. Colwell, *J. Chem. Phys.,* 1995, **103**, 10095.

[xliv] J. Tomasi, B. Mennucci, R. Cammi, *Chem. Rev.,* 2005, **105**, 2999.